Calibration of the AXAF-HRC UV/Ion shields at Osservatorio Astronomico di Palermo G.S.Vaiana: III - Synchrotron measurements of XANES in aluminum coated Lexan film samples.

M. Barbera[1], A. Collura[2,1], A. Dara[1]

[1]Istituto e Osservatorio Astronomico G.S. Vaiana
Palermo, Italy, 90134
[2]Istituto per le Applicazioni Interdisciplinari della Fisica (CNR)
Palermo, Italy 90123

ABSTRACT

High spectral resolution X-ray transmission measurements in the energy range 60-1950 eV have been conducted at BESSY 1 synchrotron (Berlin) on samples of aluminum coated Lexan in order to define an accurate model of X-ray Absorption Near Edge Structures for the AXAF-HRC UV/Ion shields material. A large number of energies have been surveyed with a spectral resolution ranging from $E/\Delta E = 2500$ at 100 eV to $E/\Delta E = 700$ at Al-K edge. The spatial variations of such absorption structures have been also investigated surveying different positions of the film samples.

KEY WORDS: X-ray, Astronomy, Instrumentation, AXAF

1 INTRODUCTION

All components of the instrumentation for X-ray detection in space astronomy (e.g. mirrors, detectors and filters) that involves photo-electric absorption are known to have fine structure features in their response in proximity of absorption edges of the component materials. These features, if not accurately known and calibrated can significantly affect the correct interpretation of observational data.[1]

In this context, a specific calibration program has been established to characterize the near edge structures of all relevant components of the High Resolution Camera (HRC)[2] of the Advanced X-ray Astrophysics Facility (AXAF).[3] Telescope response are being calibrated at the National Space Science Laboratory in Brookhaven,[4-6] while detector response is being calibrated at the Daresbury synchrotron.[7] In this paper we present results from measurements conducted at BESSY synchrotron aimed at characterizing the near edge features of the UV/Ion shields that protect the HRC microchannel plates from UV radiation and low energy ionized particles.

After that BESSY synchrotron measurements had already been completed, UV measurements conducted at the X-ray Astronomy Calibration and Testing facility (XACT) of the Osservatorio Astronomico di Palermo G.S. Vaiana[8,9] have shown an unexpected high FUV/Visible transmission of the HRC UV/Ion shield initially based on Lexan and aluminum.[10,11] These results have led to the redesign of the HRC UV/Ion shields and therefore the synchrotron measurements will be repeated on the new UV/Ion shields.

In sections 2 we describe the adopted instrumental setup and the measurements. In section 3 we report results on thickness spatial uniformity. In section 4 the near edge absorption features are presented and their possible spatial dependence is investigated. In section 5 the measured transmission are used to build an X-ray transmission model that includes the near edge features. Section 6 summarizes the main results of this work.

2 INSTRUMENTAL SETUP AND MEASUREMENTS

Measurements have been conducted in February 1996 at the station 11.31 of the Physikalisch-Technische Bundesanstalt (PTB) radiometry laboratory[12] at BESSY 1 synchrotron in Berlin (Germany). The beam-line includes a SX-700 type plane grating monochromator[13] with a useful photon energy in the range 60 - 2000 eV and spectral resolution ranging from $E/\Delta E = 2500$ at 100 eV to $E/\Delta E = 700$ at Al-K edge, and a test chamber (700 mm long, 600 mm diameter) provided with vacuum compatible micro-positioning system for samples and detectors manipulation. Two detectors have been used: a GaP/Au Schottky-type photo-diode (Hamamatsu G1963) with a sensitive area of $4.6 \times 4.6\ mm^2$ and a channel electron multiplier (VALVO X913 BL) (CEM). The photo-diode performs well and is actually used at all surveyed energies with the exception of the range 283-300 eV, where the CEM is more appropriate because of the low flux available in that region.

The three samples under study (see table 1) were mounted on a four-position fixture (one position left open) attached to a micro-positioning system allowing complete two dimensional scans of the samples. A 400 μm spot size was chosen as the best compromise between flux stability and spatial resolution.

Column 1 in table 1 gives sample number, column 2 is the manufacturer ID. number (Luxel Corporation, Friday Harbor, WA), column 3 is the sample material, column 4 gives the nominal thickness, column 5 and 6 give the Y and Z motor positions of the filters. Sample 1 is a witness sample of the AXAF HRC-I UV/Ion shield baseline design and consists of a Lexan membrane with aluminum coating on both sides. Sample 2 consists of a Lexan membrane with single side aluminum coating (previously measured at NSLS in Brookhaven[17]), and sample 3 is a Lexan membrane with no coating used to disentangle plastic and aluminum contributions to the measured X-ray transmission.

Table 2 lists the set of conducted measurements. Two dimensional spatial scans at fixed energy have been performed to locate the sample center positions and to get an insight on the sample thickness uniformity. The energy scans in the range 60-1950 eV have been conducted on three different position of sample 1 and one position on both sample 2, and 3. Table 3 describes in detail the instrumental setting of the energy scans.

Each individual measurement (i.e. each measurement at a given energy in the energy scans or each measurement at a given position in the spatial scans) is the average of 3 independent consecutive detector readings. If the readings are not consistent to each other within 1 % the measurement is automatically repeated. Each measurement is normalized by the current of the beam in the storage ring. This procedure accounts for the time dependence of the beam ensuring measurement stability at 1% level over a time scale of 30 minutes. All our measurement sets were taken over time scales shorter than 10 minutes, so to ensure no significant drift between measurements at open and at sample position.

The measurement technique described above ensures a statistical uncertainty within 1 % at all energies. Stray light contribution in the monochromatic radiation between 1.0 and 1.5 keV is up to 2 % resulting in a transmission uncertainty within 1 % for measured samples like ours. The maximum second order contamination has been measured as a function of energy and its estimate is given below[14,13]

Energy range	% Contribution
< 70 eV	0.1
70 - 150 eV	1.0
150 - 200 eV	3.0
200 - 250 eV	5.0
elsewhere	0.3

The uncertainty on measured transmission resulting from this contamination is a function of energy (E) according to the following formula:

$$\Delta T/T = \frac{c(n-1)}{1+c} \tag{1}$$

where c is the second order contamination listed in the above table and n is the ratio $T(2E)/T(E)$ for the filter under study. Figure 1 is a plot of relative (top panel) and absolute (bottom panel) uncertainties on transmission including statistical uncertainty, stray-light, and second order contamination.

3 SPATIAL THICKNESS UNIFORMITY

Figure 2 shows normalized Diode signal as a function of position along horizontal (left panel) and vertical scans (right panel) of sample 1 measured at five different energies, namely 96 eV, 140 eV, 350 eV, 541 eV, and 1700 eV.

At 96 eV where the aluminum layer transmits only 0.1 % while Lexan transmits about 10 %, transmission non-uniformity are up to 3 % (see figure 2, solid line). This allows a maximum of 0.5 % relative thickness non-uniformity of aluminum layer or 1.5 % relative non-uniformity of Lexan thickness. Thickness non-uniformity is therefore constrained, for the surveyed area, to a maximum of 0.5 % for aluminum and 1.5 % for Lexan. Measurements at the other energies do not give better constraints.

4 NEAR EDGE ABSORPTION STRUCTURES

One of the first aim of these measurements was to confirm our expectations that the fine structures in proximity of the absorption edges do not change with position on the samples, our materials being amorphous. For this purpose we have conducted transmission measurements in three different positions of sample 1. Figures 3 (left panel) and 4 show transmission vs. energy for the three surveyed positions in the energy range of aluminum, oxygen and carbon. Superimposed are the measurement uncertainties.

The small shift among the measurements conducted on the three positions of sample 1 at the aluminum edge (see figure 3 left panel) are not due to a different thickness of the aluminum layer because the measured jump ratios at the absorption edge are very close to each other. This shift is likely due to a systematic effect (likely stray-light), in fact, the three sets of measurements are consistent to each other within the error (see figure 3 left panel). Figure 3 right panel shows a plot of measured transmission for sample 1 (Pos. 1) and sample 2. The two sets of measurements have been normalized to take into account the difference in aluminum thickness. The very good agreement between these two sets of measurements taken on different samples is a further indication of position independence of aluminum near edge absorption structures. The oxygen edge shown in figure 4 left panel is also indicative of spatially even near edge absorption structure.

The case of the carbon edge shown in figure 4 right panel needs a bit more discussion. Differences observed in the first resonant peak in transmission at about 286.5 eV can be due to a small energy shift in the monochromator setting among the three set of measurements. In fact, transmission is very steep on both sides of this peak and a small energy shift can be responsible for a significant difference in transmission. Furthermore, we notice that the order of transmission values of the three positions reverses going from the left side of the peak ($T_{POS3} > T_{POS2} > T_{POS1}$) to the right side ($T_{POS1} > T_{POS2} > T_{POS3}$) of the peak. The differences observed among the three sets of measurements at the second resonant peak, located at about 291 eV, cannot indeed be interpreted in terms of an energy shift of the monochromator. The fact that transmission of the three sets of data are consistent to each other on both sides of this resonant peak suggest that observed differences cannot be accounted for by measurement uncertainties.[15] We point out in passing that the first resonant peak (consistent with spatial uniformity) is in the XANES regime (multiple scattering), while the second resonant peak (likely non spatially uniform) is in the EXAFS regime (single scattering).

5 X-RAY TRANSMISSION MODELING

The x-ray transmission of a layer of any material in the energy range 10 - 10000 eV where absorption is mainly due to the photo-electric effect is commonly modeled according to the equation

$$T(E) = e^{-\frac{\mu}{\rho}\rho t} \tag{2}$$

where ρ is the mass density of the absorbing material, μ is the linear attenuation coefficient, and t is the thickness of the layer. The mass attenuation coefficient ($\frac{\mu}{\rho}$) can be calculated from the imaginary part of the atomic scattering factors. These factors have been measured[16] for all pure atoms with coarse spacing in the entire energy range 10 - 10000 eV. The mass attenuation coefficients can also be derived for compounds according to the equation

$$\frac{\mu}{\rho} = \sum_i w_i (\frac{\mu}{\rho})_i \tag{3}$$

where w_i is the relative weight of the i_{th} element in the compound, and $(\frac{\mu}{\rho})_i$ is the mass attenuation coefficients of the i_{th} element.

Henke measurements of the imaginary part of the atomic scattering factor[16] are only coarsely spaced in energy in proximity of the absorption edges. A significant improvement of the model can be obtained[17] including in the model the absorption jumping ratios from Henke and Helgin (1970).[18] In any case, the mass attenuation coefficients derived for a compound does not take into account fine structure features that occur near the absorption edges due to interactions of the photoelectrons with the closer atoms in the molecules of the compound (XANES and EXAFS). In order to define the mass attenuation coefficients of a compound including these features, direct transmission measurements need to be conducted on the compound material of interest.

For this purpose we have conducted high spectral resolution x-ray transmission measurements of a sample of pure Lexan (sample 3) and of samples with Lexan and aluminum (sample 1 and 2). The transmission measurements outside the absorption edges (see below for the definition of the excluded energy gaps) are used to derive the mass areal density of the filter material adopting a least χ^2 fitting procedure and the model based on Henke tables.[16] The mass attenuation coefficients in the energy ranges of the absorption edges are then derived from the measured transmission and above derived mass areal density (equation 2).

5.1 Sample 3: pure Lexan

The edges of C and O in the transmission measurements of sample 3 are located at 285.5 eV and 532 eV, respectively. The energy gaps that were excluded in the fitting procedure to derive the mass areal density ρt are $281 - 360\ eV$ and $526 - 575\ eV$ for C and O, respectively. Outside these regions no significant deviation is found from the model transmission based on Henke tables.[16]

As shown in figure 1, transmission measurements at energies below 220 eV are affected by large uncertainties due to contamination from higher orders. For this reason we have also excluded these measurements in the fitting procedure to estimate the mass areal density of Lexan. Figure 5 upper panel shows the measured transmission of sample 3 with superimposed the least χ^2 fitting model. The lower panel gives the relative residuals $(T_{MEAS} - T_{FIT})/T_{MEAS}$ (dot symbols) with + symbols superimposed in correspondence to the energies included in the best fit analysis. The results of the fitting are given in table 4 line 3 (the adopted density value for Lexan is $1.2\ g/cm^3$).

5.2 Sample 1 and 2: Lexan + aluminum

The edge of Al in the transmission measurements of sample 2 is located at 1560 eV. The energy range that was excluded in the fitting procedure is $1558 - 1700\ eV$. Figure 6 upper and lower panels show the measured transmission of sample 2 with superimposed the least χ^2 fitting model, and relative residuals, respectively. Results of the fitting are given in table 4 line 2 (the density value adopted for aluminum is $2.5\ g/cm^3$).

Table 4 line 1 gives the results of the same fitting analysis conducted on sample 1. Thickness uncertainties take into account also the spatial non-uniformity of Lexan found between the three surveyed positions. The quite high value of χ^2 and indications on the presence of aluminum oxide coming from FUV/Visible measurements conducted at the XACT facility[10,11] have suggested to include aluminum oxide in the transmission model. Table 4 lines 4 and 5 report the fitting results on sample 1 and 2 when aluminum oxide is included (the density value adopted for aluminum oxide is $3.97\ g/cm^3$). Notice that the χ^2 values are significantly lower when aluminum oxide is included in the model. The amount of aluminum oxide found on sample 2 is less than half that found on sample 1. This was expected because sample 2 has aluminum coating only on one side while sample 1 has aluminum coating on both sides and thus two exposed surfaces.

Figure 7 shows the measured transmission with superimposed the least χ^2 fitting model derived including aluminum oxide and using the new set of mass attenuation coefficients derived for Lexan and aluminum. Results of this fitting are given in table 4 line 6. We note that the high χ^2 value is due to the large systematic errors of the new sets of measurements not taken into account in the χ^2 computation. The relative residuals shown in the bottom panel of figure 7 are within 2% relative at all energies except the absorption edges where the relative residuals are within 5%. A comparison of figure 7 bottom panel and figure 1 shows that at energies above 220 eV agreement between model and measurements is basically within measurement uncertainties, with the exception of few data point at the oxygen and aluminum absorption edges. At lower energies the large measurement uncertainties do not allow to state the accuracy of the model to better than 10% relative. A better knowledge of the systematic uncertainties in the conducted transmission measurements should allow to improve the accuracy of available transmission model.

6 SUMMARY AND CONCLUSIONS

We have conducted x-ray transmission measurements of Lexan and aluminum coated Lexan filters at PTB laboratory at BESSY 1 synchrotron. Three samples have been measured covering the energy range 60-1950 eV with energy resolution ranging from $E/\Delta E = 2500$ at 100 eV to $E/\Delta E = 700$ at Al-K edge.

Spatial thickness uniformity has been investigated on sample 1 in table 1. Thickness fluctuation up to 1.5 % were measured on the Lexan membrane ($\sim$ 6000 Å thick), and below 1 % on the coated aluminum layer ($\sim$ 350 Å per side).

Spatial dependence of the near edge absorption features was investigated conducting transmission measurements in three different positions of sample 1. The near edge features of oxygen and aluminum are found to be not dependent on position. The near edge features of carbon were found not dependent on position in the XANES regime. In the EXAFS regime some differences likely occur between the three surveyed positions which cannot be accounted for by measurement uncertainties.[15]

We find that taking into account the presence of aluminum oxide significantly improves the accuracy of the x-ray transmission model. An amount of aluminum oxide nearly half is found on sample 2 (single side coating) with respect to sample 1 (double side coating).

New tables of mass attenuation coefficients for Lexan and aluminum coated on Lexan are derived from the transmission measurements. The x-ray transmission model based on the derived values of mass attenuation coefficients and taking into account the presence of aluminum oxide is accurate within 2 % relative at all energies above 220 eV with the exception of the absorption edges of C, O, and Al where the accuracy is within 5% relative. At lower energies the large measurement uncertainties do not allow to state the accuracy of the model to better than 10 % relative.

New synchrotron x-ray transmission measurements are being planned for samples of the new HRC UV/Ion shield design based on Polyimide, carbon, and aluminum.

Acknowledgments

We thank Detlef Fuchs, Peter Bulicke, and Stefan Kraft of PTB laboratory at BESSY for their assistance in obtaining and analyzing this data. We acknowledge partial support from Ministero dell'Università e della Ricerca Scientifica, Agenzia Spaziale Italiana, and CNR (AC).

7 REFERENCES

[1] Owens, A., Denby, M., Wells, A., Keay, A., Graessle, D., Blake, R.L., 1995, ApJ submitted.

[2] Murray, S.S., Chappel, J.H., 1985, Proc. SPIE, 597, 274.

[3] Weisskopf, M., 1985, Proc. SPIE, 597, 228.

[4] Graessle, D.E., Clark, A.M., Fitch, J.J., Harris, B., Schwartz, D.A., Blake, R.L., 1996, these proceedings.

[5] Fitch, J.J., Graessle, D.E., Harris, B., Hughes, J.P., Nguyen, D.T., Schwartz, D.A., 1996, these proceedings.

[6] Harris, B., Graessle, D.E., Fitch, J.J., Juda, J.Z., Blake, R.L., Gullikson, E.M., 1996, these proceedings.

[7] Pearse, S.E., Lees, J.F., Pearson, J.F., Fraser, G.W., Brunton, A.N., Flanagan, K.A., Kenter, A., Barbera, M., Dhanak, V., Robinson, A., Teehan, D., 1995, SPIE proceedings, Vol. 2518, 322.

[8] Collura, A., , Barbera, M., Inzerillo, G., , Mirabello, F., Sciortino, S., Serio, S., 1994, these proceedings.

[9] Collura, A., Barbera, M., Dara, A., Inzerillo, G., , Mirabello, F., Sciortino, S., Serio, S., 1996, these proceedings.

[10] Barbera, M., Collura, A., Dara, A., Leone, M., Powell, F.R., Serio, S., Varisco, S., Zombeck, M.V., 1996, sumitted to Experimental Astronomy.

[11] Barbera, M., Collura, A., Dara, A., 1996, these proceedings.

[12] D. Fuchs, M. Krumrey, P. Muller, F. Scholze, and G. Ulm, February 1995, Rev. Sci. Instrum. 66 (2).

[13] F. Scholze, M. Krumrey, P. Muller, and D. Fuchs, October 1994, Rev. Sci. Instrum., 65 (10).

[14] Kraft Stefan, PTB laboratory, BESSY 1, Private communication

[15] Fuchs Detlef, PTB laboratory, BESSY 1, Private communication

[16] Henke, B.L., Gullikson, E.M., and Davis, J.C., 1993, Atomic Data and Nuclear Data tables, Vol. 54, No. 2, July 1993.

[17] Barbera, M., Breslau, D., Flanagan, K., Graessle, D., Zombeck, M.V., 1994, SPIE proc., Vol. 2280, ?????.

[18] Henke, B.L., & Elgin, R.L., 1970, Advances in X-ray Analysis, vol. 13, Plenum Press, NY.

TABLES AND FIGURES

Table 1: List of Measured Film Samples

Sample	ID. Num.	Material	Nominal Thickness (Å) Al	Lexan	Al	Y	Z
1	TF101-952	Al-Lexan[1]-Al	360±35	6065±100	345±35	0	28, 35, 33.1
2	TF101-542	Al-Lexan[1]	710±50	5805±100		0	72.9
3	TF110-380	Lexan[1]		5740±100		0	113.1

[1]General Electric RL5002.

Table 2: List of Conducted Measurements

Horizontal scan	(Z= 0, 150 mm)	of the 3 samples	at energy 350 eV
Horizontal scan	(Z= 23, 45 mm)	of sample #1	at 350 eV
Vertical scan	(Y= -12, +12 mm)	of sample #1	at 350 eV
Horizontal scan	(Z= 66, 78 mm)	of sample #2	at 350 eV
Vertical scan	(Y= -8, +8 mm)	of sample #2	at 350 eV
Horizontal scan	(Z= 103, 125 mm)	of sample #3	at 350 eV
Vertical scan	(Y= -12, +12 mm)	of sample #3	at 350 eV
Energy scan	(60-1950 eV)	of sample #1	at (Z= 28.0 mm, Y=0 mm)
Energy scan	(60-1950 eV)	of sample #1	at (Z= 35.0 mm, Y=0 mm)
Energy scan	(60-1950 eV)	of sample #1	at (Z= 33.1 mm, Y=0 mm)
Energy scan	(60-1950 eV)	of sample #2	at (Z= 72.9 mm, Y=0 mm)
Energy scan	(60-1950 eV)	of sample #3	at (Z=113.1 mm, Y=0 mm)
Horizontal scan	(Z= 23, 45 mm)	of sample #1	at 1700 eV
Vertical scan	(Y= -12, +12 mm)	of sample #1	at 1700 eV
Horizontal scan	(Z= 23, 45 mm)	of sample #1	at 140 eV
Vertical scan	(Y= -12, +12 mm)	of sample #1	at 140 eV
Horizontal scan	(Z= 23, 45 mm)	of sample #1	at 541 eV
Vertical scan	(Y= -12,+12 mm)	of sample #1	at 541 eV
Horizontal scan	(Z= 23, 45 mm)	of sample #1	at 96 eV
Vertical scan	(Y= -12, +12 mm)	of sample #1	at 96 eV

Table 3: Energies Surveyed in the Transmission Measurements

Filter	Energy range (eV)	energy step (eV)	Absorption Edge
Beryllium 0.25 μm	60 – 71	1	
Beryllium 0.25 μm	71.2 – 75	0.2	Aluminum LII,LIII
Beryllium 0.25 μm	76 – 110	1	
No Filter	100 – 250	2	
Titanium 1 μm	250 – 280	2	
Titanium 1 μm	280.5 – 293	0.5	Carbon K
Titanium 1 μm	295 – 450	5	
Iron 0.5 μm	450 – 520	2	
Iron 0.5 μm	521 – 529	1	
Iron 0.5 μm	529.2 – 540	0.2	Oxygen K
Iron 0.5 μm	541 – 565	1	
Iron 0.5 μm	570 – 700	5	
Copper 0.5 μm	700 – 900	5	
Berrylium 7 μm	900 – 1540	10	
Berrylium 7 μm	1542 – 1600	2	Aluminum K
Berrylium 7 μm	1605 – 1700	2	
Berrylium 7 μm	1710 – 1950	10	

Table 4: Best Fit results on synchrotron x-ray transmission measurements

Sample	Mass Areal Density ($\mu g\ cm^{-2}$)			Derived Thickness (Å)			χ^2
	Al	Lexan	Al_2O_3	Al	Lexan	Al_2O_3	
1	18.2±0.2	75 ± 2		730±10	6290±100		3.17
2	15.2±0.2	71.9±0.6		610±10	5990±30		1.48
3		74.0±0.6			6170±30		1.48
1	15.7±0.2	74 ± 2	4.4±0.4	630±10	6160±100	110±10	1.04
2	14.2±0.2	71.3±0.6	1.7±0.4	570±10	5940±30	40±10	1.18
1	15.1±0.2	74 ± 2	5.2±0.4	600±10	6180±100	130±10	18.1

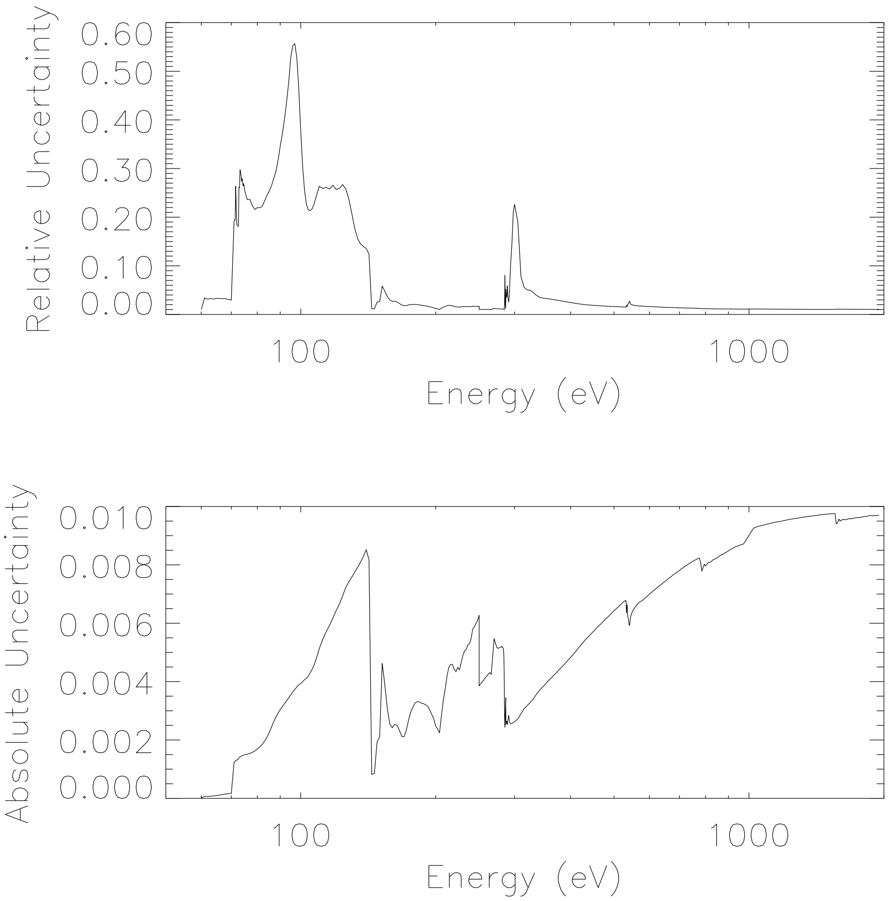

Figure 1: Relative uncertainties (top panel) and absolute uncertainties (lower panel) in the transmission measurements as a function of energy.

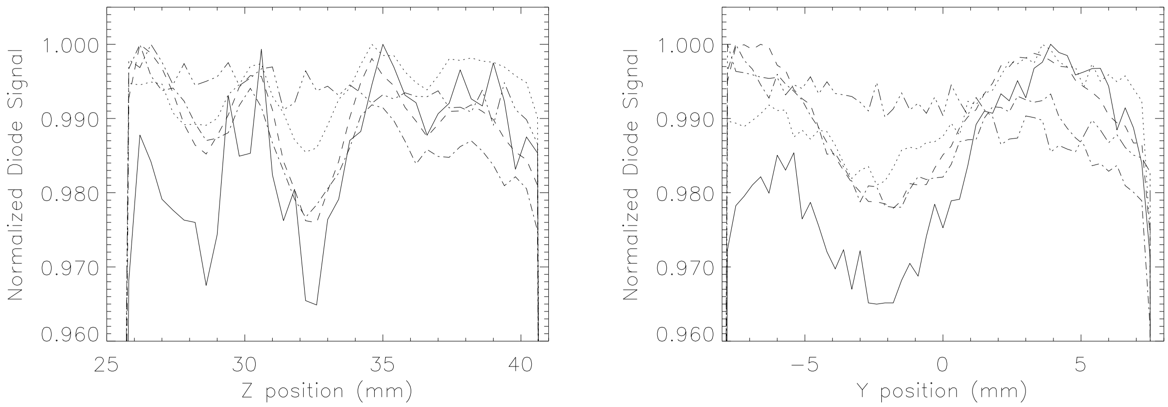

Figure 2: Normalized diode signal as a function of position along horizontal (left panel) and vertical scans (right panel) of sample 1 measured at five different energies, namely 96 eV (solid line), 140 eV (dotted line), 350 eV (dashed line), 541 eV (dash-dot line), 1700 eV (dash-dot-dot-dot line).

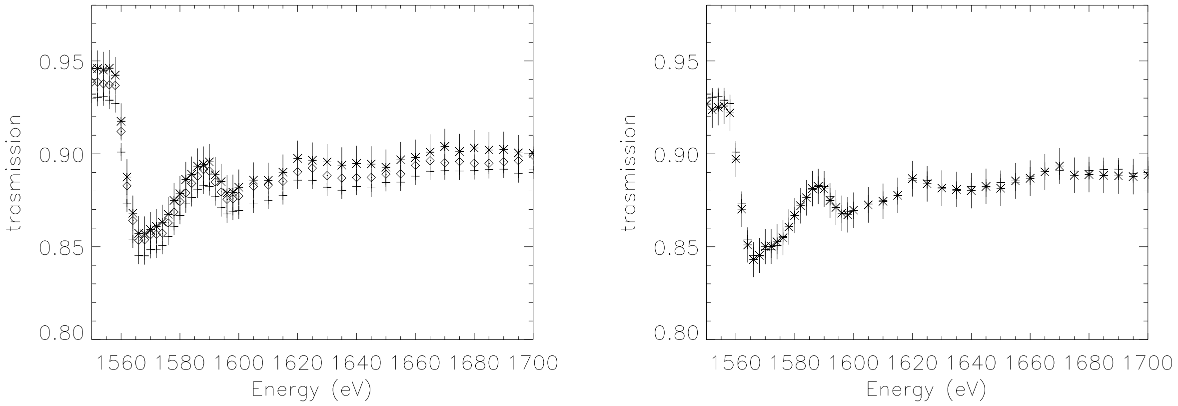

Figure 3: Left panel is the transmission vs. energy at the aluminum absorption edge for the three surveyed position of sample 1, namely position 1 (Z=28 mm, plus symbols), position 2 (Z=35 mm, asterisk symbol), position 3 (Z=33.1 mm, square symbol). Right panel is the same plot for sample 1 position 1 (plus symbols) and sample 2 asterisk symbol). Superimposed are the measurement uncertainty including systematic uncertainty due to higher order contamination

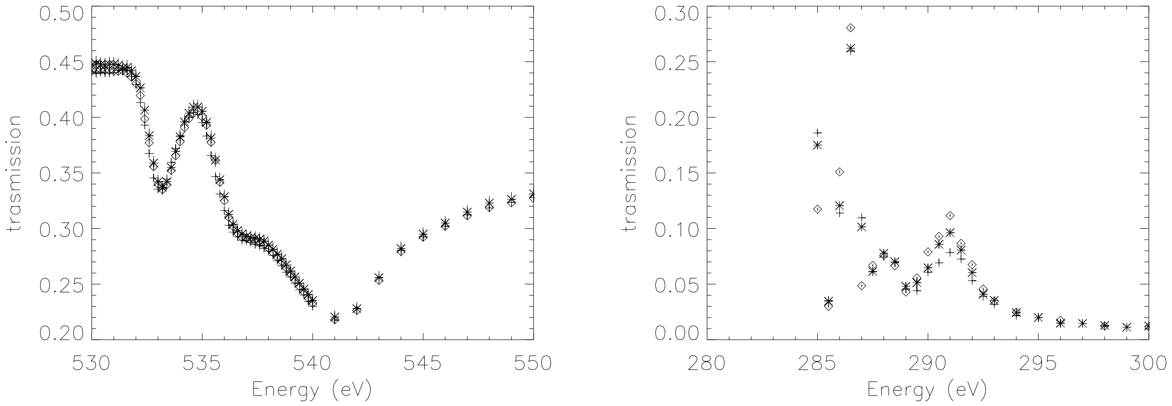

Figure 4: Transmission vs. energy for the three surveyed position of sample 1 at the oxygen absorption edge (left panel), and at the carbon absorption edge (right panel). Superimposed are the measurement uncertainties.

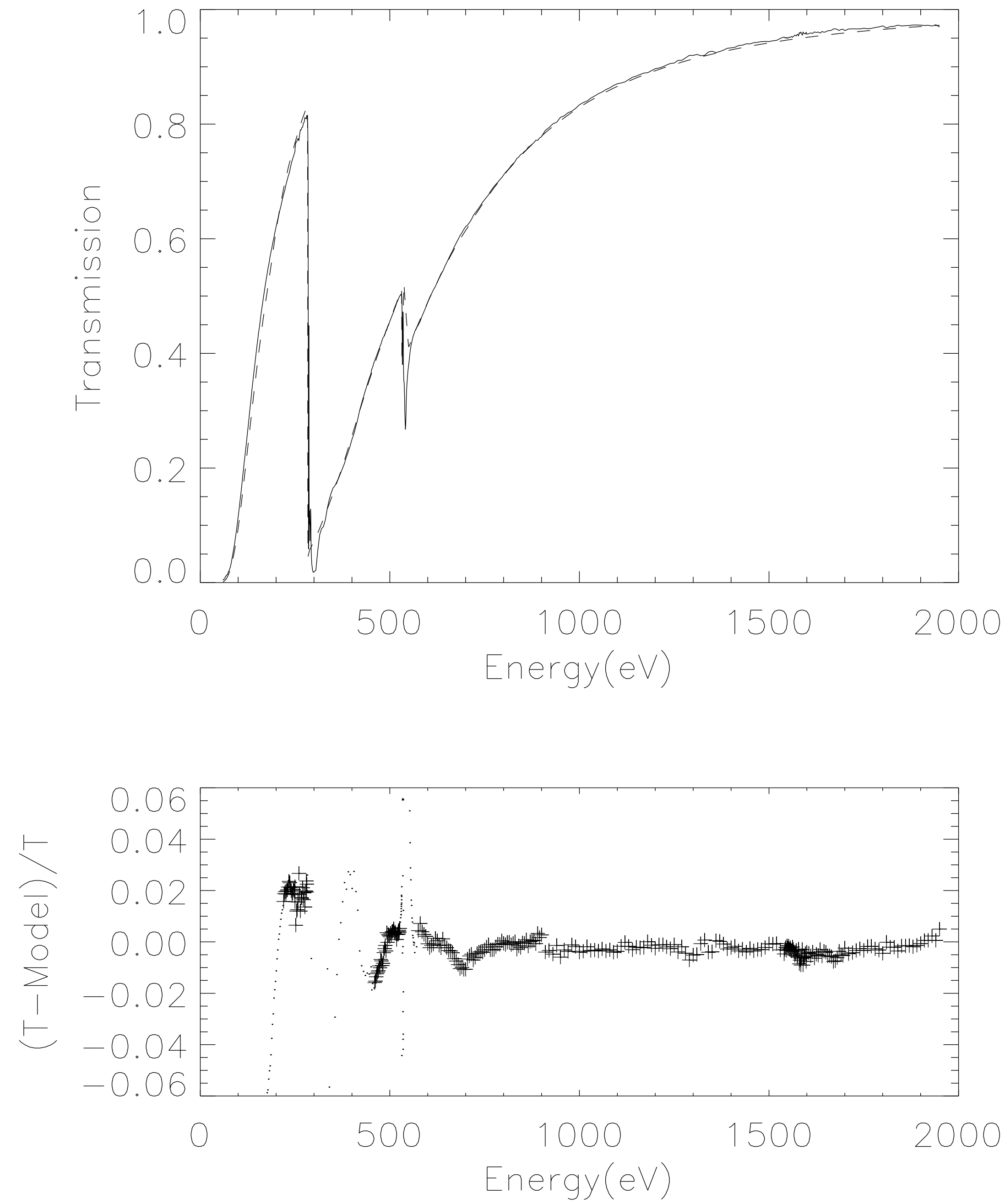

Figure 5: Measured transmission vs. energy for a sample of pure Lexan (sample 3) together with the least χ^2 fit conducted on measurements which do not include the energy regions of C and O absorption edges (Top panel). The bottom panel gives the relative residuals $(T_{MEAS} - T_{FIT})/T_{MEAS}$ (dot symbols) with + symbols over-plotted at the energies included in the least χ^2 fitting procedure.

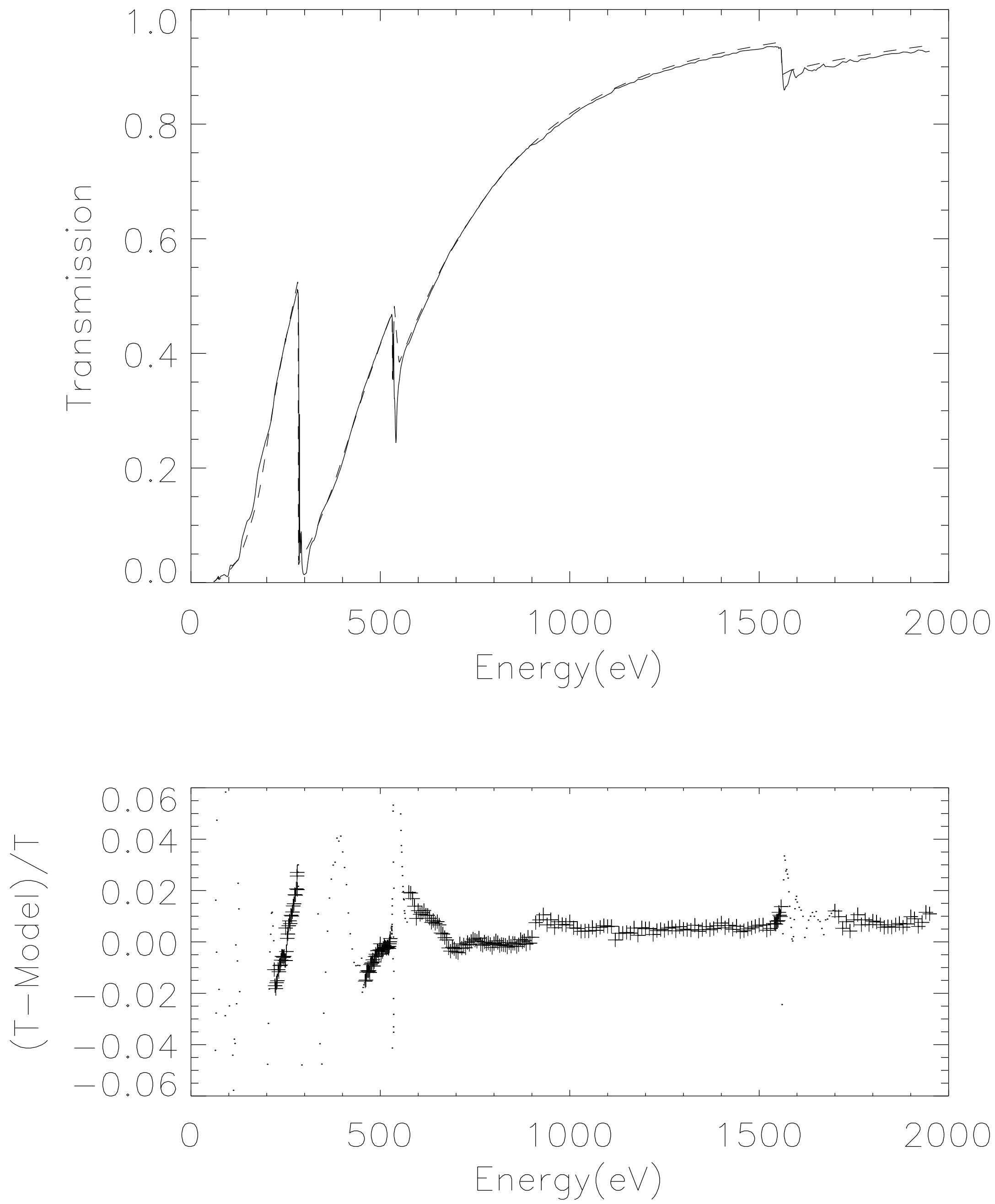

Figure 6: Measured transmission vs. energy for a sample of aluminum coated Lexan (sample 2) together with the least χ^2 fit conducted on measurements which do not include the energy regions of C and O absorption edges (Top panel). The bottom panel gives the relative residuals $(T_{MEAS} - T_{FIT})/T_{MEAS}$ (dot symbols) with + symbols over-plotted at the energies included in the least χ^2 fitting procedure.

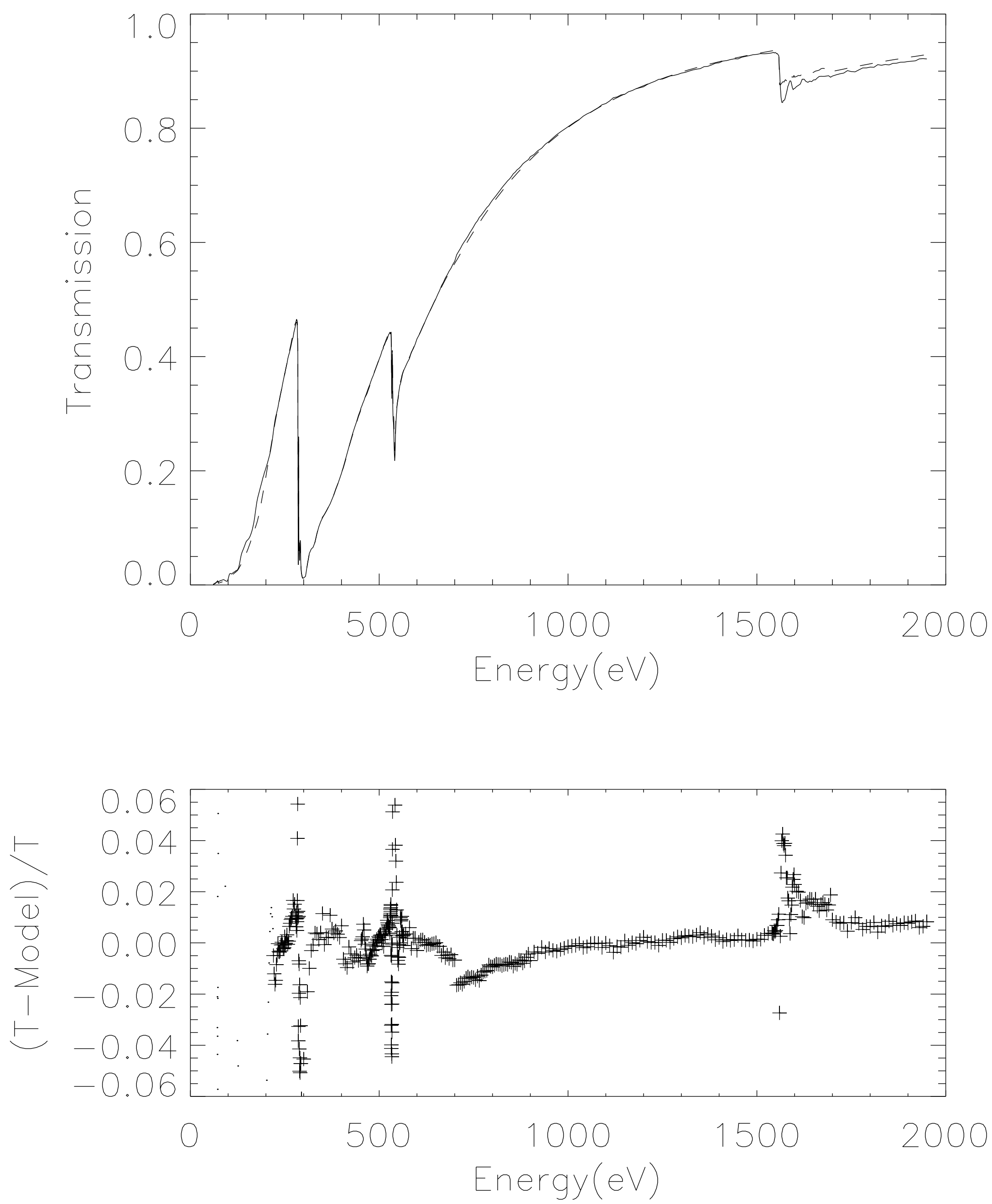

Figure 7: Measured transmission vs. energy for a sample of aluminum coated Lexan (sample 1) together with the least χ^2 fit conducted on measurements including the energy regions of C, O, and Al absorption edges (Top panel). The bottom panel gives the relative residuals $(T_{MEAS} - T_{FIT})/T_{MEAS}$ (dot symbols) with + symbols over-plotted at the energies included in the least χ^2 fitting procedure.